

Received: 2019.05.20
Accepted: 2019.07.29
Published: 2019.11.18

A Nude Mouse Model of Orthotopic Liver Transplantation of Human Hepatocellular Carcinoma HCCLM3 Cell Xenografts and the Use of Imaging to Evaluate Tumor Progression

Authors' Contribution:
Study Design A
Data Collection B
Statistical Analysis C
Data Interpretation D
Manuscript Preparation E
Literature Search F
Funds Collection G

ABCDEF 1,2 **Zhi-ting Xu**
ABCDEFG 1 **Hong Ding**
ADEF 1,2 **Tian-tian Fu**
ABE 1 **Yu-li Zhu**
ABE 1 **Wen-ping Wang**

1 Department of Ultrasound, Zhongshan Hospital, Fudan University, Shanghai, P.R. China
2 Shanghai Institute of Medical Imaging, Shanghai, P.R. China

Corresponding Author: Hong Ding, e-mail: ding.hong@zs-hospital.sh.cn
Source of support: This study was supported by the National Natural Science Fund (No. 81571675, and No. 81873897)

Background: This study aimed to develop a nude mouse model of orthotopic liver transplantation of HCCLM3 human hepatocellular carcinoma (HCC) cell xenografts and the use of imaging and histology to evaluate tumor development and progression.

Material/Methods: HCCLM3 cells were injected subcutaneously into 25 healthy male athymic BALB/c (nu/nu) nude mice. The tumors that developed were transplanted into the liver of a new set of nude mice. After four weeks and six weeks, the mice were imaged using ultrasound (US), software-assisted contrast-enhanced ultrasound (CEUS), fluorodeoxyglucose-positron emission tomography (FDG-PET). Histology was performed on the liver and liver tumors, and included immunohistochemistry for vascular endothelial growth factor (VEGF), CD31, CD34, and α -smooth muscle actin (α -SMA).

Results: The success rate for orthotopic tumor transplantation in the mouse liver was 90% (18/20). Liver tumors measured 11.8 ± 2.6 mm in diameter and 525.9 ± 250.8 mm³ in volume on the sixth week. CEUS showed rapid wash-in and washout in the liver tumors, and PET showed low tumor cell metabolism. Bone metastases were present in 45% (9/20) of mice in the sixth week. Immunohistochemistry showed positive expression for VEGF, CD31, CD34, and α -SMA.

Conclusions: The nude mouse orthotopic liver transplantation model of human HCC was shown to be a reliable model that has the potential for future research on the pathogenesis and progression of HCC and studies on drug development.

MeSH Keywords: **Carcinoma *in Situ* • Carcinoma, Hepatocellular • Mice, Nude • Models, Animal**

Full-text PDF: <https://www.medscimonit.com/abstract/index/idArt/917648>

 2618  2  7  31



Background

Worldwide, hepatocellular carcinoma (HCC) is the most common type of liver cancer and the third leading cause of cancer death [1]. Chronic liver diseases, especially cirrhosis, are the main risk factors for HCC [2]. Treatment for HCC is usually limited because most patients with HCC are diagnosed at an advanced stage. Surgical resection, targeted therapy, immunotherapy, and systemic chemotherapy are among the current treatments for HCC. Due to molecular heterogeneity and chromosomal alterations, the molecular mechanism of HCC remain unclear, and therapeutic options still needed to be developed [3].

Development of new treatments for cancer, including drug development, requires initial preclinical analysis. The use of stable and reliable animal models that have similar characteristics to the human disease is required for *in vivo* preclinical drug development studies. Currently, nude mice have been identified as suitable for these studies, and there have now been several different types of HCC nude mouse models [4,5]. The orthotopic tumor transplantation model using nude mice has been reported to be a close model for primary human HCC [6]. However, because of the high technical requirements and the need for the use of immunodeficient nude mice as hosts, these animal models have yet to be extensively used.

Ultrasound (US) is a useful screening method to detect tumor development, and contrast-enhanced ultrasound (CEUS) uses real-time imaging technology. CEUS can evaluate the tumor characteristics, including tumor size, vascular invasion, and growth patterns, and has the potential to identify therapeutic responses [7]. Fluorodeoxyglucose-positron emission tomography (FDG-PET) is an effective method for the diagnosis of cancer and monitors tumor glucose metabolism.

Therefore, this study aimed to develop a nude mouse model of orthotopic liver transplantation of HCCLM3 human HCC cell xenografts with the use of imaging and histology to evaluate tumor development and progression.

Material and Methods

Cell culture

The human hepatocellular carcinoma HCC cell line, HCCLM3 [8], was established at the Liver Cancer Institute, Zhongshan Hospital, Fudan University, Shanghai. The cells with the highest metastatic potential were subcultured and maintained in Dulbecco's modified Eagle's medium (DMEM) (Biosera, Boussens, France) supplemented with 10% fetal bovine serum (FBS) (Biosera, Boussens, France). All cells were incubated at

37°C in a humidified atmosphere containing 5% CO₂. The doubling time of the HCCLM3 cells was calculated, and the cell count was performed. The cells were maintained in culture for four passages before inoculation into the mice, to ensure cell viability and stability,

Establishment of the HCCLM3 tumor xenografts in the nude mice

Twenty-five healthy male athymic BALB/c (nu/nu) nude mice were purchased from the SLAC Laboratory Animal Co., Ltd. (Shanghai, China). The mice were 6 weeks old and weighed 18–20 g. The mice were housed and fed in a specific pathogen-free (SPF) environment and provided with sterile food and water. All procedures were performed under aseptic condition. Before the animal experiments, the mice were fed *ad libitum* for one week in the new environment.

Cultured cells were washed with phosphate-buffered saline (PBS) (Biosera, Boussens, France), and 0.2 mL of cell suspension (1×10^7 cells) was injected into the skin of the right underarm region of five nude mice.

Orthotopic liver transplantation of the human HCCLM3 tumor xenografts in the nude mice

Two weeks later, when the xenograft tumors were about 1 cm³ in volume, the tumor tissues were removed from the subcutaneous site in each of the mice. The tumors were cut into pieces measuring 2 mm in diameter and transplanted into the subcapsular region of the left medial lobe of the liver of a different set of 20 nude mice. A gelatin sponge was applied to the site, and the liver incision was sutured using 8-0 nylon surgical sutures (Ethicon Inc., Johnson & Johnson, New Brunswick, NJ, USA) with local disinfection. During the operation, intraperitoneal anesthesia using 2% pentobarbital sodium (40 mg/kg) was administered. At the end of the study, the mice were euthanized when the liver tumors reached about 20 mm in length.

Evaluation of the growth of the orthotopic liver tumors

After orthotopic liver transplantation, all mice were imaged each week using a Philips EPIQ 7 US system (Philips, Amsterdam, the Netherlands) with an L12-4 convex probe (4–12MHz). The focus depth and other settings remained unchanged and were constant during the study.

The liver tumor dimensions were measured using ultrasound. The orthotopic liver tumor volume was calculated using the following formula: $V = \text{length} \times \text{width} \times \text{height} / 2$. The tumor length and width were measured in the horizontal plane, and the depth was measured in the sagittal plane.



Figure 1. Two weeks after subcutaneous injection of the HCCLM3 human hepatocellular carcinoma cells into the nude mice, tumor xenograft nodules were present. Two weeks after subcutaneous injection of the HCCLM3 human hepatocellular carcinoma cells, a subcutaneous tumor nodule is shown in the right underarm of the nude mouse (diameter=10 mm).

When the liver tumors increased to 5 mm in length, a 100-second imaging record using contrast-enhanced ultrasound (CEUS) dynamic imaging was acquired using after injection of 150 μ L of re-suspended microbubble contrast (SonoVue, Bracco, Milan, Italy) into the tail vein of the mice. Quantitative imaging software was used to draw the time-intensity curve (TIC). Other imaging parameters included the peak intensity (PI), and area under the curve (AUC), which were calculated for both the liver tumor and the adjacent liver parenchyma. The metabolism of the liver tumor and metastases was evaluated using fluorodeoxyglucose-positron emission tomography (FDG-PET). Standardized uptake values (SUVs) of the tumor tissue were calculated using computer software.

Tumor histopathology and immunohistochemistry

At the end of the study, immediately after CEUS was performed, liver and tumor tissue specimens were fixed in 10% neutral buffered formalin, embedded in paraffin wax, and tissue sections were cut. Tumor tissue sections underwent immunohistochemistry using primary antibodies to vascular endothelial growth factor (VEGF), CD31, CD34, and α -smooth muscle actin (α -SMA). All light microscopy images were digitized, and the images were analyzed using Panoramic 1000 image analysis software (3DHistech, Budapest, Hungary).

Statistical analysis

Numerical data were presented as the mean \pm standard deviation (SD). Simple linear regression models were applied to analyze the morphological changes of the tumor with time,



Figure 2. Gray-scale ultrasound (US) imaging shows the orthotopic liver transplant of the hepatocellular carcinoma (HCC) xenograft at the fourth week. Gray-scale ultrasound (US) imaging shows a 7.79 \times 5.78 mm hypoechoic nodule in the left lobe of the liver of the nude mouse at the fourth week after orthotopic liver transplantation.

including both the diameter and volume. All statistical analysis was performed using SAS version 10.0 software (SAS Software, Cary, NC, USA). A P-value <0.05 was considered to be statistically significant.

Results

The nude mouse model of orthotopic liver transplantation of human HCCLM3 hepatocellular carcinoma (HCC) tumor xenografts

Two weeks after subcutaneous implantation of HCCLM3 cells, xenograft tumors appeared in 4/5 (80%) nude mice without metastasis (Figure 1). Three weeks after orthotopic liver transplantation of the tumor xenografts, liver tumor growth was detected by ultrasound (US) in 18/20 (90%) nude mice (Figure 2), and positron emission tomography (PET) showed that bone metastasis was present in 9/20 (45%) nude mice (Figure 3).

Tumor growth of the orthotopic HCC liver tumors

The orthotopic liver tumors were evaluated during the third week when they were 4.2 ± 0.5 mm in diameter and 22.4 ± 7.3 mm³ in volume. On the sixth week, at the end of the study, the orthotopic liver tumors measured 11.8 ± 2.6 mm in diameter and 525.9 ± 250.8 mm³ in volume (Figure 4, Table 1).

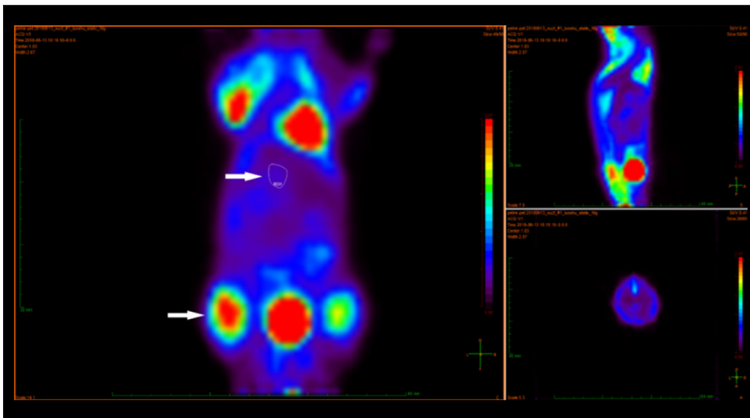


Figure 3. Positron emission tomography (PET) shows bone metastasis in the mouse at the sixth week. The upper arrow indicates tumor tissue. The lower arrow indicates metastasis in the right femur in the sixth week.



Figure 4. The orthotopic liver tumors were evaluated during the third week and sixth week.

Contrast-enhanced ultrasound (CEUS)

On the fourth week after orthotopic transplantation, CEUS imaging showed homogeneous enhancement with hyper-echogenicity at 5 ± 1 s after injection of microbubble contrast (SonoVue, Bracco, Milan, Italy) (Figure 5A). Following washout, medium echogenicity was found at 10 ± 2 s (Figure 5B), and washout hypo-echogenicity was found during the portal and delayed phase (Figure 5C). At the sixth week after orthotopic transplantation, uneven hypo-enhancement was found at 6 ± 1 s after injection of microbubble contrast (SonoVue, Bracco,

Milan, Italy) (Figure 5D). After washout, there was a lack of echogenicity at 10 ± 2 s until the delayed phase (Figure 5E).

The time-intensity curves (TICs) of the mouse liver tissue, including the liver tumor and liver parenchyma, were evaluated by quantitative image analysis software (Figures 6A, 6B). The peak intensity (PI), and area under the curve (AUC) decreased (Table 2). Positron emission tomography (PET) in the sixth week after orthotopic liver transplantation showed a maximum standardized uptake value (SUV) of 0.38 ± 0.04 . Metastasis to the femur was present in 9/20 (45%) mice.

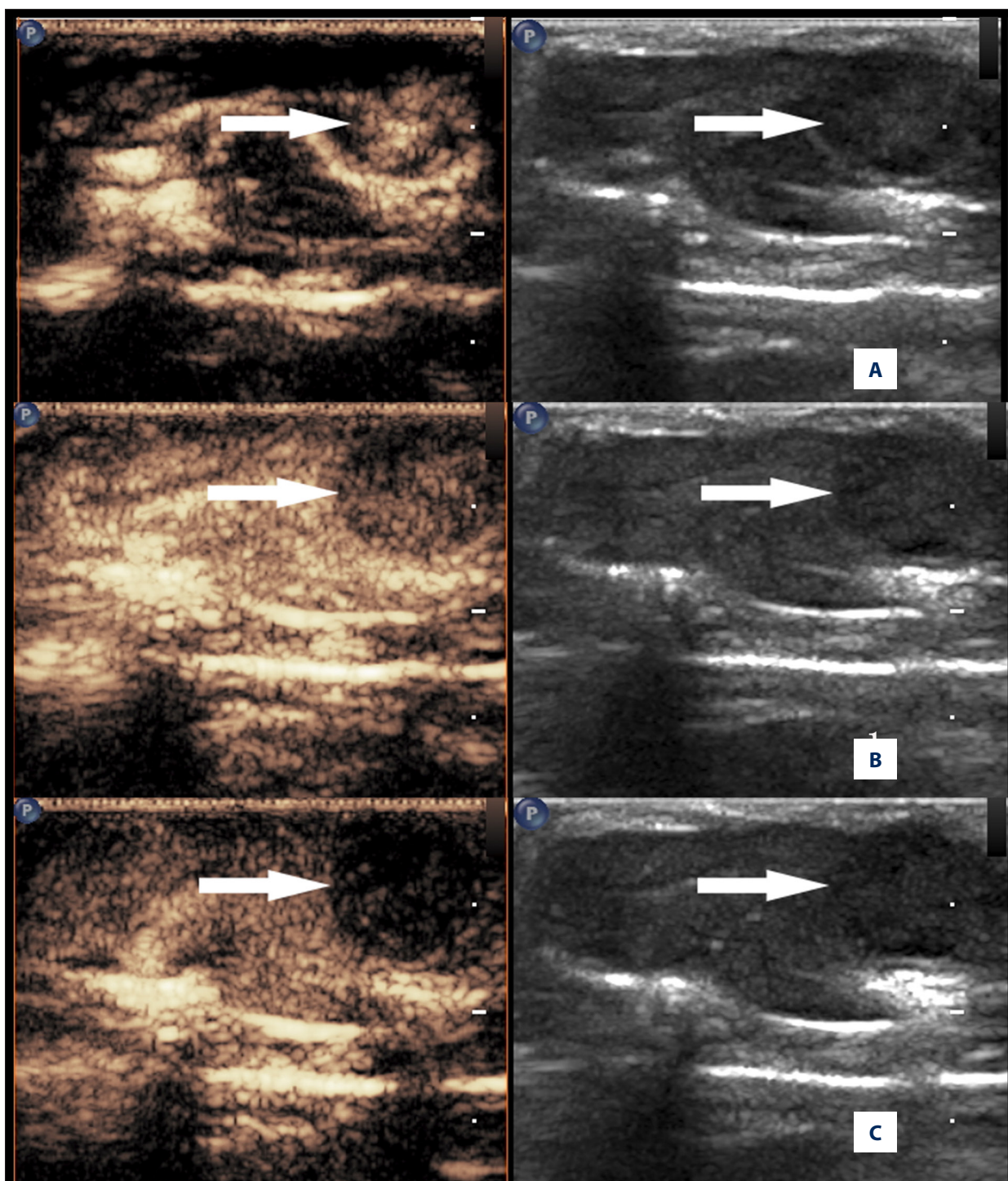
Histology and immunohistochemistry of the mouse liver tissue and the orthotopically transplanted liver tumors

Vascular invasion of the orthotopically transplanted HCC was determined by immunohistochemistry for vascular endothelial growth factor (VEGF) (Figure 7A), and α -smooth muscle actin (α -SMA) (Figure 7B). The microvessel density (MVD) index was determined using immunostaining for CD31 (Figure 7C) and CD34 (Figure 7D). Histology confirmed that the tumors in the mouse liver tissues and the metastases showed features of HCC, which were associated with areas of necrosis.

Table 1. The morphological features of the mouse tumor xenografts in the third, fourth, fifth, and sixth week after orthotopic liver transplantation of the tumor xenograft.

	n	Weeks after transplantation				Linear regression coefficient	P-value
		3 rd week	4 th week	5 th week	6 th week		
Tumor diameter (mm)	18	4.2 ± 0.5	5.9 ± 1.0	9.1 ± 1.8	11.8 ± 2.6	0.7517	<0.0001
Tumor volume (mm ³)	18	22.4 ± 7.3	77.6 ± 53.0	249.6 ± 188.4	525.9 ± 250.8	0.5675	<0.0001

n – number of orthotopic liver tumors.



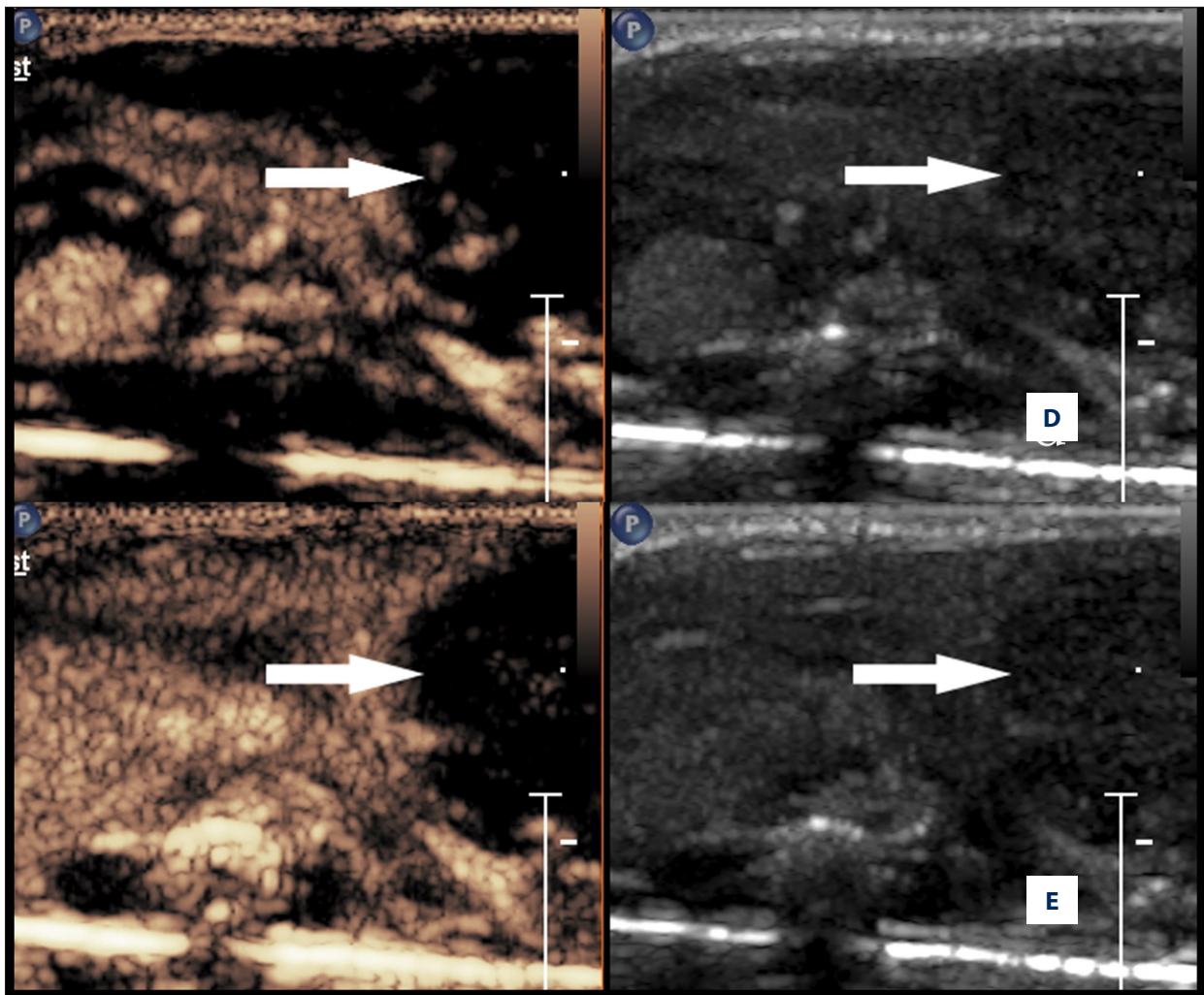


Figure 5. Contrast-enhanced ultrasound (CEUS) in the fourth week and sixth week after orthotopic liver transplantation of the hepatocellular carcinoma tumor xenograft. (A) Contrast-enhanced ultrasound (CEUS) imaging shows homogeneous enhancement with hyperechogenicity at 5 ± 1 s after injection of microbubble contrast (the fourth week after orthotopic liver transplantation of tumor xenograft). (B) Following washout, medium echogenicity was found at 10 ± 2 s (the fourth week after orthotopic liver transplantation of tumor xenograft). (C) Medium echogenicity is shown at washout during the portal and delayed phase (the fourth week after orthotopic liver transplantation of tumor xenograft). (D) Uneven hypo-enhancement is shown at 6 ± 1 s after injection of microbubble contrast (SonoVue, Bracco, Milan, Italy) (the sixth week after transplantation). (E) After washout, there is a lack of echogenicity at 10 ± 2 s until the delayed phase (the sixth week after transplantation).

Discussion

Worldwide, hepatocellular carcinoma (HCC) accounts for approximately 80% of primary malignant liver cancers [9]. Tumor angiogenesis occurs in HCC and has recently been targeted in personalized therapy for HCC. However, the mechanisms underlying the role of angiogenesis in HCC remain poorly understood. In this study, the nude mouse orthotopic liver transplantation model of human HCC was shown to be reliable in terms of tumor development and progression. This model may be helpful for future research on the molecular

mechanisms of tumor initiation, growth, angiogenesis, and drug development.

Previously used models in human malignancy have included tumor xenografts, the use of spontaneous tumor models, viral-induced animal tumors, and genetically-engineered animal models [10]. Of these five methods, the tumor xenograft animal model is the most widely used. However, in HCC, the success rate of establishing human HCC cell lines is low and is reported to be less than 25% [11,12]. The use of human HCC cell lines is characterized by rapid cell proliferation *in vitro*, and

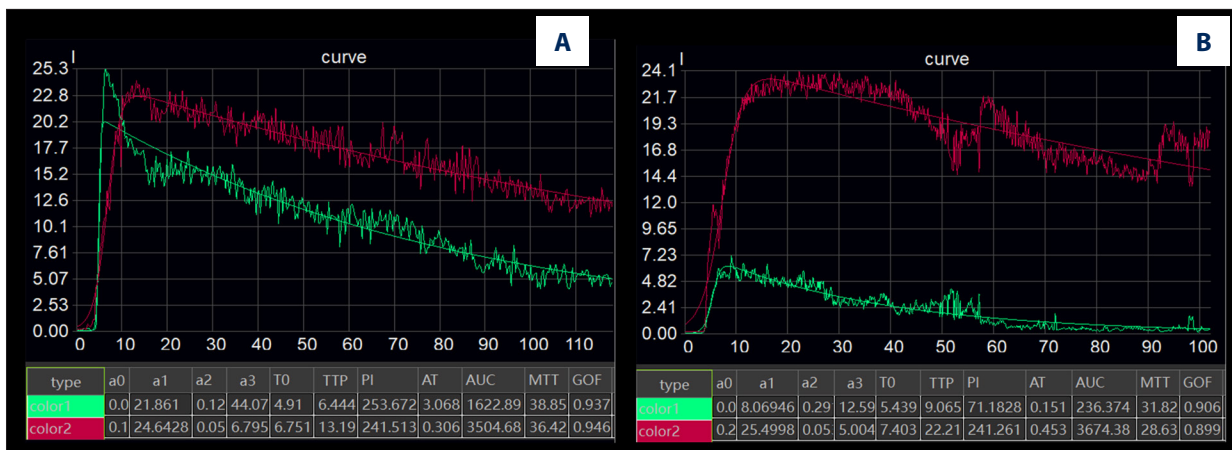


Figure 6. The time-intensity curves of the mouse liver tissue histology including the liver tumor and liver parenchyma in the fourth and sixth week. **(A)** Time-intensity curve of the liver tumor tissue (green line) and the liver parenchyma (red line) in the fourth week. **(B)** Time-intensity curve of the liver tumor tissue (green line) and the liver parenchyma (red line) in the sixth week.

Table 2. Quantified parameters used in contrast-enhanced ultrasound (CEUS).

Weeks after transplantation	Liver tissue sections	PI	AUC
4 th week	Tumor	256.4±46.1	2853.4±1459.6
	Parenchyma	290.3±39.4	4660.2±1835.9
5 th week	Tumor	192.2±68.6	1873.4±1168.3
	Parenchyma	294.2±67.4	4655.3±1469.4
6 th week	Tumor	152.4±54.5	1028.7±696.7
	Parenchyma	272.2±61.3	3759.2±759.3

PI – peak intensity; AUC – area under the curve. Parenchyma selected is of the same depth as the tumor tissue.

their use in animal HCC xenografts results in tumors at injection sites and sometimes in metastatic tumors in the peritoneal cavity [11,12]. The success rates for this approach could be improved by optimizing the cell culture environment to improve cell viability to >70% and to reduce contact inhibition while in culture [11]. Another approach is to use a xenograft in an ideal animal model that would be more stable than cell lines used from human surgical tumor tissue explants [13]. Therefore, in this study, we chose the human HCC cell line, HCCLM3, to develop the model, because of its high cell proliferation rate *in vitro*, which was reflected by the tumor growth and metastatic potential *in vivo* [8].

In addition to orthotopic liver transplantation of tumor xenografts, other technologies include injection of cell suspensions into the portal vein, or the hepatic artery, the spleen, or subcutaneous tumor implants. The spleen is an appropriate site for xenograft tumor growth because it is highly vascularized and has space to accommodate tumor growth. However, with the use of HCC xenografts, partial hepatectomy has been shown to increase the success rate regardless of the site [14]. Regarding

the animal model, mice share a similar genetic, anatomical, and immune system with humans [15]. The immune-deficient thymectomized nude mouse and the nonobese diabetic/severe combined immunodeficiency (NOD/SCID) mouse have been used in previous models [16,17]. The BALB/c mouse is hairless, which is convenient for both tumor observation and imaging [18]. In the mouse, the underarm and back have a rich blood supply [19], which are ideal regions for subcutaneous implantation of tumor xenografts.

In this study, several imaging techniques were used to follow the development of transplanted tumors. In the advanced stage of tumor development in this model, both blood perfusion and the systemic circulation decreased, indicating tumor necrosis. Ultrasound (US) is a reproducible and accurate screening tool for early HCC, which may present as hypoechoic, isoechoic, or hyperechoic areas when compared with the surrounding liver tissue. On its basis, the use of contrast-enhanced ultrasound (CEUS) has been recommended by the World Federation for Ultrasound in Medicine and Biology (WFUMB) and the European Federation of Societies for Ultrasound in Medicine and Biology (EFSUMB) [20],

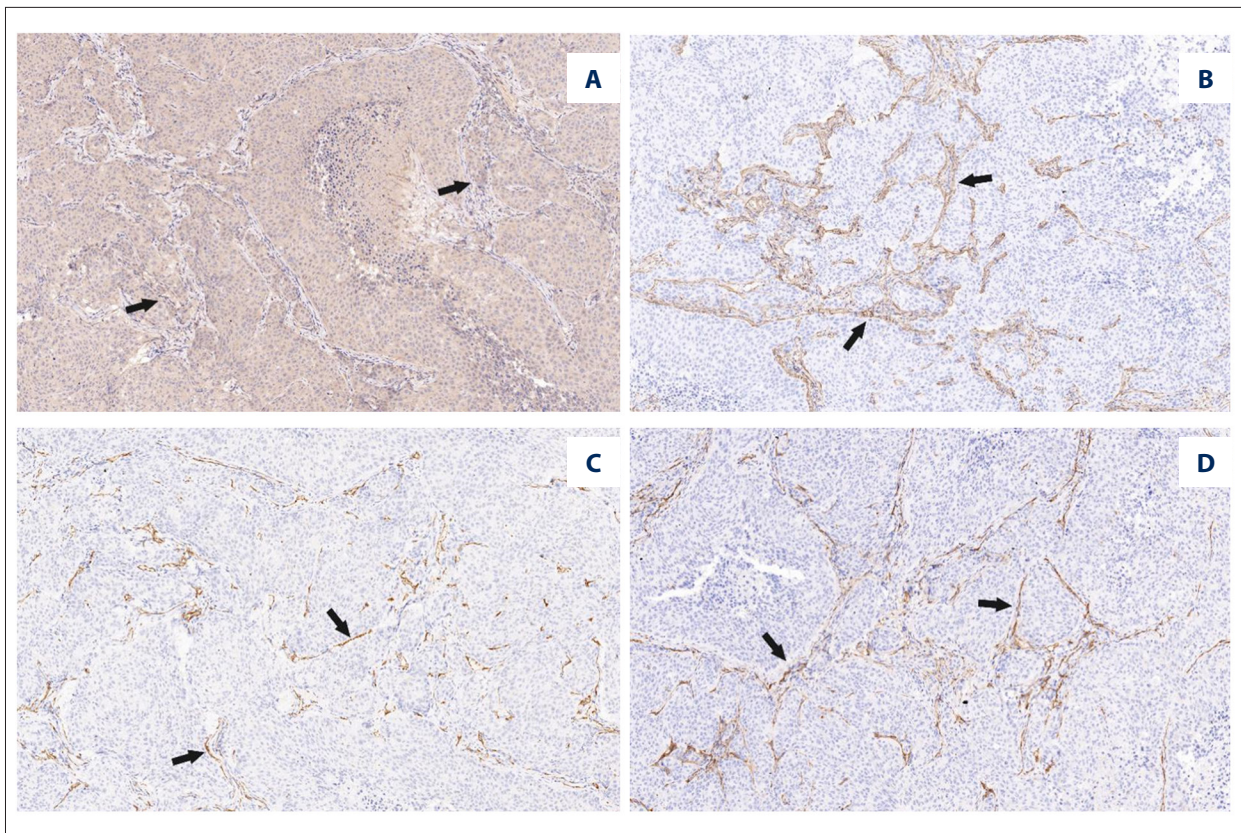


Figure 7. Photomicrographs of the histology and immunohistochemistry of the mouse liver tissue and the orthotopic liver tumor transplantation. **(A)** Immunohistochemistry shows the localization of vascular endothelial growth factor (VEGF) expression around the nests of cancer cells (brown). (Original magnification, $\times 200$). **(B)** Immunohistochemistry shows the localization of α -smooth muscle actin (α -SMA) expression around the fibroblasts and myofibroblasts (brown). (Original magnification, $\times 200$). **(C)** Immunohistochemistry shows the localization of CD31 expression in the tumor tissue microvessels (brown), located between the malignant cells. The microvessel density (MVD) index could be calculated from the immunostaining. (Original magnification, $\times 200$). **(D)** Immunohistochemistry shows the localization of CD34 (brown), with an expression pattern similar to CD31, but with stronger immunopositivity. The microvessel density (MVD) index could be calculated from the immunostaining. (Original magnification, $\times 200$).

for the diagnosis of focal liver lesions using contrast imaging. The typical CEUS imaging appearance of HCC is enhancement during the arterial period, together with rapid washout of the contrast agent during the portal venous or late period [21]. These findings are consistent with the imaging appearance found in the HCC mouse model reported in the present study. In the HCC mouse model, peak intensity (PI), and area under the curve (AUC) were the two parameters which reflected the blood perfusion volume. However, the sensitivity of positron emission tomography (PET) for the diagnosis of HCC is only about 50% [22], and the standardized uptake values (SUVs) are lower when the tumor size is smaller. However, PET but be used to scan the whole body to detect metastases. Other imaging techniques that are also suitable for use in animal xenograft models include X-rays, computed tomography (CT), and magnetic resonance imaging (MRI). In 2017, Li et al. [23] used synchrotron radiation-based X-ray imaging in a similar liver tumor model and analyzed tissue characteristics and neovascularization without

the use of contrast agent. This imaging method obtained a clear tumor microvascular density and included 3D reconstruction of tumor samples, with detection of vessels as small as $20 \mu\text{m}$ [23]. However, this imaging method may not be suitable for clinical use due to the high levels of radiation involved.

HCC is a hypervascular malignancy. Detection of vascular endothelial growth factor (VEGF) and measurement of microvessel density (MVD), are commonly used to evaluate HCC. VEGF expression promotes tumor angiogenesis, mitogenesis, and vascular permeability [24]. Tumor recurrence and metastasis may also be predicted by measuring the expression levels of VEGF [25]. CD31 and CD34 are endothelial antigens that facilitate endothelial cell adhesion and are also markers for angiogenesis in malignant tumors [26,27]. Also, α -smooth muscle actin (α -SMA) is a marker for vascular maturation and integrity and is present in the stromal fibroblasts and myofibroblasts of solid tumors, including HCC [28].

The major technical innovation of the animal model presented in this study is the use of the liver orthotopic xenografts, derived from a human HCC cell line, which were initially grafted in the mouse subcutaneous tissue. The advantages of this approach include the short experimental period, good reproducibility, high tumorigenicity, and similar biological characteristics between the liver tumors and human HCC. This model also included the development and progression of the HCC from tumor growth, to angiogenesis and tumor invasion, to metastasis to sites that included bone. Therefore, this model has the potential for future studies in tumor biology, the effects of carcinogens, and the effects of potential anti-cancer agents during drug development, including molecular targeted therapy and immunotherapy. In the past decade, studies have used similar mouse models to evaluate the efficacy, toxicity, and dosing of new drugs [29,30]. In this study, we demonstrated that this model could be used in combination with real-time vascular imaging technology using CEUS.

However, this study had several limitations. In the study period used, the model showed metastases to bone but did not develop other systemic metastases; for example, in the lung [31]. Also, we selected highly aggressive cells from the human HCCLM3 HCC cell line. The mice were at an early age,

which might have influenced tumor development. Other factors that might have influenced the model include the duration of the cell passages, which could have been reduced, and the duration of the study (six weeks), as a more extended study period may have resulted in more systemic metastases. Also, the use of immunodeficient mice that do not have the native characteristics of humans with HCC may have affected tumor behavior. Further studies should be conducted to examine the effects on this model of varying the duration of cell passage, the duration of the study, and the use of different human HCC cell lines that have a range of cell differentiation and malignant behavior.

Conclusions

This study aimed to develop a nude mouse model of orthotopic liver transplantation of HCCLM3 human hepatocellular carcinoma (HCC) cell xenografts and the use of imaging and histology to evaluate tumor development and progression. The nude mouse orthotopic liver transplantation model of human HCC was shown to be a reliable model that has the potential for future research on the pathogenesis and progression of HCC and studies on drug development.

References:

- Bray F, Ferlay J, Soerjomataram I et al: Global cancer statistics 2018: GLOBOCAN estimates of incidence and mortality worldwide for 36 cancers in 185 countries. *Cancer J Clin*, 2018; 68(6): 394–424
- Balogh J, Victor DR, Asham EH et al: Hepatocellular carcinoma: A review. *J Hepatocell Carcinoma*, 2016; 3: 41–53
- Hoshida Y, Toffanin S, Lachenmayer A et al: Molecular classification and novel targets in hepatocellular carcinoma: Recent advancements. *Semin Liver Dis*, 2010; 30(1): 35–51
- Sun FX, Tang ZY, Liu KD et al: Establishment of a metastatic model of human hepatocellular carcinoma in nude mice via orthotopic implantation of histologically intact tissues. *Int J Cancer*, 1996; 66(2): 239–43
- Shimosato Y, Kameya T, Nagai K et al: Transplantation of human tumors in nude mice. *J Natl Cancer Inst*, 1976; 56(6): 1251–60
- Hoffman RM: Orthotopic is orthodox: Why are orthotopic-transplant metastatic models different from all other models? *J Cell Biochem*, 1994; 56(1): 1–3
- Lencioni R, Llovet JM: Modified RECIST (mRECIST) assessment for hepatocellular carcinoma. *Semin Liver Dis*, 2010; 30(1): 52–60
- Li Y, Tang Y, Ye L et al: Establishment of a hepatocellular carcinoma cell line with unique metastatic characteristics through *in vivo* selection and screening for metastasis-related genes through cDNA microarray. *J Cancer Res Clin Oncol*, 2003; 129(1): 43–51
- McGlynn KA, Petrick JL, London WT: Global epidemiology of hepatocellular carcinoma: An emphasis on demographic and regional variability. *Clin Liver Dis*, 2015; 19(2): 223–38
- Wu L, Tang Z, Li Y: Experimental models of hepatocellular carcinoma: developments and evolution. *J Cancer Res Clin Oncol*. 2009; 135(8): 969–81.
- Cheung PF, Yip CW, Ng LW, et al. Establishment and characterization of a novel primary hepatocellular carcinoma cell line with metastatic ability *in vivo*. *Cancer Cell Int*, 2014; 14(1): 103
- Qiu Z, Zou K, Zhuang L et al: Hepatocellular carcinoma cell lines retain the genomic and transcriptomic landscapes of primary human cancers. *Sci Rep*, 2016; 6: 27411
- Rheinwald JG, Beckett MA: Tumorigenic keratinocyte lines requiring anchorage and fibroblast support cultured from human squamous cell carcinomas. *Cancer Res*, 1981; 41(5): 1657–63
- Ahmed SU, Zair M, Chen K et al: Generation of subcutaneous and intrahepatic human hepatocellular carcinoma xenografts in immunodeficient mice. *J Vis Exp*, 2013; (79): e50544
- Bernardi R, Grisendi S, Pandolfi PP: Modelling haematopoietic malignancies in the mouse and therapeutic implications. *Oncogene*, 2002; 21(21): 3445–58
- Yan M, Li H, Zhao F et al: Establishment of NOD/SCID mouse models of human hepatocellular carcinoma via subcutaneous transplantation of histologically intact tumor tissue. *Chin J Cancer Res*, 2013; 25(3): 289–98
- Suetsugu A, Katz M, Fleming J et al: Multi-color palette of fluorescent proteins for imaging the tumor microenvironment of orthotopic tumorgraft mouse models of clinical pancreatic cancer specimens. *J Cell Biochem*, 2012; 113(7): 2290–95
- Szadvari I, Krizanova O, Babula P: Athymic nude mice as an experimental model for cancer treatment. *Physiol Res*, 2016; 65(Suppl. 4): S441–53
- Watanabe T, Morizane T, Tsuchimoto K et al: Establishment of a cell line (HCC-M) from a human hepatocellular carcinoma. *Int J Cancer*, 1983; 32(2): 141–46
- Claudon R, Dietrich CF, Choi BI et al: Guidelines and good clinical practice recommendations for contrast enhanced ultrasound (CEUS) in the liver; Update 2012: A WFUMB-EFSUMB initiative in cooperation with representatives of AFSUMB, AIUM, ASUM, FLAUS and ICUS. *Ultraschall Med*, 2013; 34(1): 11–29
- Lencioni R, Piscaglia F, Bolondi L: Contrast-enhanced ultrasound in the diagnosis of hepatocellular carcinoma. *J Hepatol*, 2008; 48(5): 848–57
- Hectors SJ, Wagner M, Besa C et al: Multiparametric FDG-PET/MRI of hepatocellular carcinoma: initial experience. *Contrast Media Mol Imaging*, 2018; 2018: 5638283
- Li B, Zhang Y, Wu W et al: Neovascularization of hepatocellular carcinoma in a nude mouse orthotopic liver cancer model: A morphological study using X-ray in-line phase-contrast imaging. *BMC Cancer*, 2017; 17(1): 73

24. Yano T, Tanikawa S, Fujie T et al: Vascular endothelial growth factor expression and neovascularisation in non-small cell lung cancer. *Eur J Cancer*, 2000; 36(5): 601–9
25. Yamaguchi R, Yano H, Nakashima O et al: Expression of vascular endothelial growth factor-C in human hepatocellular carcinoma. *J Gastroenterol Hepatol*, 2006; 21(1): 152–60
26. Pusztaszeri MP, Seelentag W, Bosman FT: Immunohistochemical expression of endothelial markers CD31, CD34, von Willebrand factor, and Fli-1 in normal human tissues. *J Histochem Cytochem*, 2006; 54(4): 385–95
27. Mineo TC, Ambrogi V, Baldi A et al: Prognostic impact of VEGF, CD31, CD34, and CD105 expression and tumour vessel invasion after radical surgery for IB-IIA non-small cell lung cancer. *J Clin Pathol*, 2004; 57(6): 591–97
28. Parikh JG, Kulkarni A, Johns C: α -smooth muscle actin-positive fibroblasts correlate with poor survival in hepatocellular carcinoma. *Oncol Lett*, 2014; 7(2): 573–75
29. Baron Toaldo M, Salvatore V, Marinelli S et al: Use of VEGFR-2 targeted ultrasound contrast agent for the early evaluation of response to sorafenib in a mouse model of hepatocellular carcinoma. *Mol Imaging Biol*, 2015; 17(1): 29–37
30. Matsuki M, Hoshi T, Yamamoto Y et al: Lenvatinib inhibits angiogenesis and tumor fibroblast growth factor signaling pathways in human hepatocellular carcinoma models. *Cancer Med*, 2018; 7(6): 2641–53
31. Gao Y, Chen X, Li K, Wu Z: Nude mice model of human hepatocellular carcinoma via orthotopic implantation of histologically intact tissue. *World J Gastroenterol*, 2004; 10(21): 3107–11